A Free Energy Perturbation Study of Solvation in Hydrazine and Carbon Tetrachloride

B. G. Rao and U. C. Singh*

Contribution from the Department of Molecular Biology, Scripps Clinic and Research Foundation, La Jolla, California 92037. *Received November 13, 1990*

Abstract: A free energy perturbation study of solvation in hydrazine and carbon tetrachloride is carried out to examine the process of solvation of different solutes in these two solvents. For this purpose, models of liquid hydrazine and liquid carbon tetrachloride were generated by molecular dynamics simulations. The structure of liquid hydrazine obtained from the molecular dynamics simulation is discussed in detail. Differences in the free energies of solvation of different solutes belonging to different classes of ions and molecules have been determined. The solutes studied include closed shell ions, tetraalkylammonium ions, normal alkanes, and tetraalkylmethane molecules. The calculated differences in free energy of solvation, ΔG, between two different solutes in these solvents compare well with the experimental values. Detailed analysis of the solvation behavior in these solvents and their comparison with the behavior of solvation in water suggest that solvation behavior in hydrazine resembles that in water for many solutes, whereas the behavior in carbon tetrachloride is different. The results of this study support the view that the special phenomenon observed in the hydration of apolar solutes is a result of the structural peculiarity of liquid water.

Introduction

As a part of our on-going research on solvation in different solvents using the free energy perturbation method, we have been investigating the characteristics of solvation of a variety of solutes in several solvents. Earlier, we reported[1,2] in this journal the results of such solvation studies in water, methanol (MeOH), and dimethyl sulfoxide (DMSO). In addition to demonstrating the usefulness of the free energy perturbation method[3] in calculating differences in the free energies of solvation in three different solvents, the work reported in the two papers has brought out several important differences between the solvation of neutral alkanes and tetraalkylammonium ions in aqueous and nonaqueous media. We have shown that the patterns of free energy variation, ΔG, with the mutation parameter, λ, for the apolar solutes in water is dictated by the reorganization of the tightly bound solvent cage around these solutes in water, in addition to the change in the solute–solvent interaction energies. Even when the polarization energy is included explicitly for the calculation of free energies,[4] the trends in the variation patterns of ΔG with λ showed a behavior similar to that noted earlier. Such a behavior is not observed in MeOH in spite of the close resemblance between this liquid and water. The same is found to be true for solvation in DMSO as well. It appears from these results that the hydration of apolar solutes is different from solvation of these solutes in nonaqueous solvents and the hydrophobic hydration results primarily from some unique features of water. The unique structural features of water as a cause of hydrophobic effect have been emphasized since the early work of Frank and Evans[5]. Several later studies[6-8] of hydrophobic effect emphasize the structural aspects of water. On the other hand, the studies[9] with scaled particle theories suggested that water is unique in its behavior due to its smaller molecular size and not due to its special structural features. A recent study[10] analyzing the data from extensive computer simulation studies on several liquids shows that hydrophobic hydration is a consequence of special structural features of water and is not due to the smaller size of water as suggested by scaled particle theories. This study has compared the "work of formation of hard spherical cavities of atomic size" in six molecular solvents which include *n*-hexane, *n*-dodecane, and *n*-undecyl alcohol, chloroform, carbon tetrachloride, and water. Our studies so far have compared water with methanol and dimethyl sulfoxide. The relative importance of the molecular size of water may be examined by a comparison of the behavior of solvation in water with that in a liquid such as hydrazine, which is extensively hydrogen bonded in the liquid state, but its molecular size is larger than that of water.

Table I. Some Properties of Water, Hydrazine, and CCl_4

property	H_2O	hydrazine	CCl_4
mol wt, g/mol	18.015	32.042	153.823
bp, °C	100.0	113.5	76.638
mp, °C	0.0	1.8	-23.0
density, g/cm^3	0.997	1.00	1.58436
dielectric constant	78.3	51.7	2.238
dipole moment, D	1.82	1.83	0.0
viscosity, cP	0.89	0.9	0.9
surface tension, dyn cm^{-1}	71.81	66.67	26.15
trouton constant, cal deg^{-1} mol^{-1}	26.0	25.23	22.14

Hydrazine, which was labeled as inhibited "water" by Frank,[11] has close similarity with water in several of the physical and molecular properties.[12] Some of these properties are given in Table I. The liquid ranges (melting points and boiling points), densities, dipole moments, surface tensions, and trouton constants for the two liquids are nearly identical. The properties of water that differ dramatically from those of hydrazine or other solvents are the isobaric expansibility up to 4 K above the melting point and the temperature coefficient of the isothermal compressibility up to 46 K above the melting point.[13] It has been reasoned by Frank[11] that hydrazine could reproduce the properties of water that originate in its extensive hydrogen bonding but not those properties that result from changes in the unique structure of water. The gas-phase solubility data[14] bring out some of the differences between the two liquids. The Gibbs free energies of transfer of apolar solutes like argon and nitrogen from cyclohexane to water and hydrazine are very much similar but the enthalpies and entropies are different.[15] Similar results were obtained for micellization in these two liquids.[15] These studies suggest that

(1) Rao, B. G.; Singh, U. C. *J. Am. Chem. Soc.* **1989**, *111*, 3125.
(2) Rao, B. G.; Singh, U. C. *J. Am. Chem. Soc.* **1990**, *112*, 3803.
(3) For a review of recent applications using free energy perturbation methods, see: (a) Beveridge, D. L.; DiCupa, F. M. *Annu. Rev. Biophys. Biophys. Chem.* **1989**, *18*, 431. (b) Jorgensen, W. L. *Acc. Chem. Res.* **1989**, *22*, 184. (c) Kollman, P. A.; Merz, K. M., Jr. *Acc. Chem. Res.* **1990**, *23*, 246.
(4) Ramnarayan, K.; Rao, B. G.; Singh, U. C. *J. Chem. Phys.* **1990**, *92*, 7057.
(5) Frank, H. S.; Evans, M. W. *J. Chem. Phys.* **1945**, *13*, 507.
(6) (a) Pratt, L. R.; Chandler, D. *J. Chem. Phys.* **1977**, *67*, 3683. (b) Pratt, L. R. *Annu. Rev. Phys. Chem.* **1985**, *36*, 433.
(7) Mirejovsky, D.; Arnett, E. M. *J. Am. Chem. Soc.* **1983**, *105*, 1112.
(8) Muller, N. *Acc. Chem. Res.* **1990**, *23*, 23.
(9) Lee, B. *Biopolymers* **1985**, *24*, 813. Lee, B. *J. Chem. Phys.* **1985**, *83*, 2421.
(10) Pohorille, A.; Pratt, L. R. *J. Am. Chem. Soc.* **1990**, *112*, 5066.
(11) Frank, H. S. Unpublished, cited in ref 15.
(12) Organic Solvents: Physical Properties and Methods of Purification. In *Techniques of Chemistry*; Riddick, J. A., Bunger, W. B., Sakano, T. K., Eds.; John Wiley & Sons: New York, 1986; Vol. II.
(13) Marcus, Y. *Introduction to Liquid State Chemistry*; John Wiley & Sons: New York, 1977; p 113.
(14) Chang, E.; Gocken, N.; Poston, T. *J. Phys. Chem.* **1968**, *72*, 638.
(15) Ramadan, M. Sh.; Evans, D. F.; Lumry, R. *J. Phys. Chem.* **1983**, *87*, 4538.

0002-7863/91/1513-4381$02.50/0

hydrophobic properties of water and hydrazine are very similar. However, the experimental data for solvation in liquid hydrazine are very limited so far and no such data are available for larger hydrophobic solutes such as alkanes and tetraalkylammonium ions. In the present study, we intend to investigate the solvation of larger hydrophobic solutes in hydrazine by the free energy perturbation approach to find out if the solvation process in hydrazine is different from that in water. If any differences are observed between the two solvents, it should be possible from the free energy variation patterns to find out if such differences are a consequence of the structural differences of the two solvents. For this reason, we simulated the structure of liquid hydrazine by molecular dynamics to understand its similarities and differences with the structure of water.

Additionally, we study the solvation behavior in carbon tetrachloride (CCl_4), which is a nonpolar and nonassociated liquid. The solvation behavior in CCl_4 is expected to be remarkably different from that in water and hydrazine. Some of its properties[12] listed in Table I are very different from those of water or hydrazine. Nevertheless, increased gauche population of *n*-butane observed[16] in dilute CCl_4 solutions has been attributed to solvophobicity of this liquid based on RISM and computer simulation studies.[17,18] However, the results of these studies must be viewed with caution as they were found to be model dependent.[18] For instance, in one of the simulation studies by Bigot and Jorgensen[19] the increased gauche population of butane in CCl_4 was not predicted. Similarly, the ability of the infinite dilution HNC-RISM theory to correctly describe the changes in solvent structure and thermodynamics that occur when an apolar solute is placed into water is also questioned.[18] Such limitations of other macroscopic theories such a scaled particle theory in calculating thermodynamic properties of solutions have also been pointed out.[10] Therefore, a detailed microscopic simulation at the atomic level including explicitly all the interaction between the solute and solvent molecules is essential to resolve some of the contradictory conclusions drawn from the theoretical studies of solvation in liquid CCl_4.

In the present study, we consider explicitly all the atoms of all solute and solvent molecules. In addition to obtaining the structure of liquid hydrazine, we employed the free energy perturbation method to study the following transformations ion hydrazine and CCl_4: (1) $Cl^- \rightarrow Br^-$, (2) $Na^+ \rightarrow K^+$, (3) $Me_4N^+ \rightarrow NH_4^+$, (4) $Et_4N^+ \rightarrow Me_4N^+$, (5) $C_2H_6 \rightarrow CH_4$, and (6) $Me_4C \rightarrow CH_4$. Since ionic solutes are expected to be insoluble in CCl_4, it is not appropriate to study transformations 1–4 in this solvent. However, the calculations for transformations 1 and 2 in CCl_4 were carried out for the purpose of comparison only. Transformations 3 and 4 were not simulated in CCl_4. The results of the first two transformations are expected to bring out the differences in solvation of anions and cations in these solvents. The last four transformations, which brought out important differences between solvation in water and MeOH or DMSO, should give insights into the differences between water and hydrazine as well. These results of the present study are compared with those of our earlier studies.[1,2]

The Free Energy Perturbation Method

The free energy perturbation method[20] is employed in the present study. This method and its implementation into the AMBER program have been described in detail earlier.[21] Briefly, in the free energy perturbation approach, the free energy difference between two states of a system is computed by transforming one state into the other by changing a single coupling parameter in several steps. For instance, the two states, A and B, represented by Hamiltonians, H_A and H_B, are coupled by a dimensionless parameter, λ, as

$$H_\lambda = \lambda H_A + (1 - \lambda)H_B \qquad 0 \le \lambda \le 1 \tag{1}$$

When $\lambda = 1$, $H_\lambda = H_A$ and when $\lambda = 0$, $H_\lambda = H_B$. Therefore, state A can be smoothly transformed to state B by changing the value of λ in small increments, $\Delta\lambda$, such that the system is in equilibrium at all values of λ. At any intermediate value of λ, the state of the system is a hypothetical mixture of A and B.

The Gibbs free energy contribution due to the perturbation at every value of λ is given by

$$G_\lambda = -\frac{1}{\beta} \ln \langle \exp(-\beta H_\lambda) \rangle_0 \tag{2}$$

where $\beta = 1/RT$. The average of $\exp(-\beta H_\lambda)$ is computed over the unperturbed ensemble of the system. If the perturbation from $\lambda = 1$ to 0 is carried over N intervals, then the total free energy change equals the sum over all these intervals

$$\Delta G = \sum_{i=1}^{N} G_1(\lambda_i) \tag{3}$$

To circumvent some sampling difficulties during transformation, it is advantageous to decouple ΔG into two parts: an electrostatic part, ΔG_{ele}, and a van der Waals part, ΔG_{vdw}. The ΔG_{ele} represents the free energy change due to the mutation of the partial charges, whereas the ΔG_{vdw} represents the free energy change due to the mutation of the size of the molecule. This is achieved by transforming state A to state B through an intermediate state A′ such that only the partial charges are mutated during the first part of the transformation (A → A′) and the van der Waals parameters are mutated during the second part of the transformation (A′ → B). Further, the technique of coordinate coupling is applied during the mutation of the van der Waals parameters. The details of these methods are described in our earlier paper.[1]

Computational Details

All calculations were carried out with the AMBER (Version 3.1) program.[22] The details of the protocol used in the computation of the free energy differences with this program are discussed in earlier papers.[1,2] A few modifications made for simulations with solvent boxes other than water were also described.[2]

Potential Functions. Hydrazine is a unique molecule because of the lone pairs of electrons on the two nitrogen atoms, which are connected by a covalent bond in this molecule. The quantum mechanical studies on this molecule showed that the rotational barrier about the N–N bond is dictated by the lone pair–lone pair interaction which causes splitting of the lone pair energy levels. Thus, the minimum energy configuration of the hydrazine molecule is attained when the two lone pairs are perpendicular to each other, which is the gauche conformation of the molecule.[23] We have generated the potential function, $V(\phi)$, for the internal rotation around the N–N bond of hydrazine by ab inito quantum mechanical method using the 6-31G**/MP3 level and fitted it to a four-term series given in the equation below.

$$V(\phi) = \frac{1}{2}\sum_{k=1}^{4} V_k(1 - \cos k\,\phi) \tag{4}$$

ϕ is the tetrahedral angle between the two NH_2 groups (or the bisectors of the two HNH angles). The coefficients V_1, V_2, V_3, and V_4 are −5.640, −5.664, −2.056, and 0.240 kcal/mol, respectively. The values of these coefficients agree well with those reported in an earlier calculation.[24] A plot of the potential function is shown in Figure 1. The parameters of this potential function for the rotational barrier was incorporated into the molecular mechanics force field used in the calculations. Since the rotational barrier potential of hydrazine includes 1,4 interactions of the atoms attached to the nitrogen atoms, these interactions (which include both van der Waals and electrostatic interactions) were not included in the calculation of the total energy. The partial charges for the atoms of hydrazine were obtained by the ab initio program QUEST[25] with a 6-31G*

(16) Rosenthal, L.; Rabolt, J. F.; Hummel, J. *J. Chem. Phys.* **1982**, *76*, 817.
(17) Zichi, D. A.; Rossky, P. J. *J. Chem. Phys.* **1986**, *94*, 1712.
(18) Tobias, D. J.; Brooks, C. L., III *J. Chem. Phys.* **1990**, *92*, 2582.
(19) Bigot, B.; Jorgensen, W. L. *J. Chem. Phys.* **1981**, *75*, 1944.
(20) Zwanzig, R. W. *J. Chem. Phys.* **1954**, *22*, 1420.
(21) Singh, U. C.; Brown, F. K.; Bash, P. A.; Kollman, P. A. *J. Am. Chem. Soc.* **1987**, *109*, 1607.
(22) AMBER (Version 3.1) is a fully vectorized version of AMBER (Version 3.0) by Singh, U. C.; Weiner, P. K.; Caldwell, J. W.; Kollman, P. A.; University of California: San Francisco, 1986. AMBER (Version 3.1) also includes coordinate coupling and intra/inter decomposition.
(23) Jones, K. In *Comprehensive Inorganic Chemistry*; Trotman-Dickenson, A. F., Ed.; 1973; Vol. 2, p 250.
(24) Riggs, N. V.; Radom, L. *Aust. J. Chem.* **1986**, *39*, 1917.

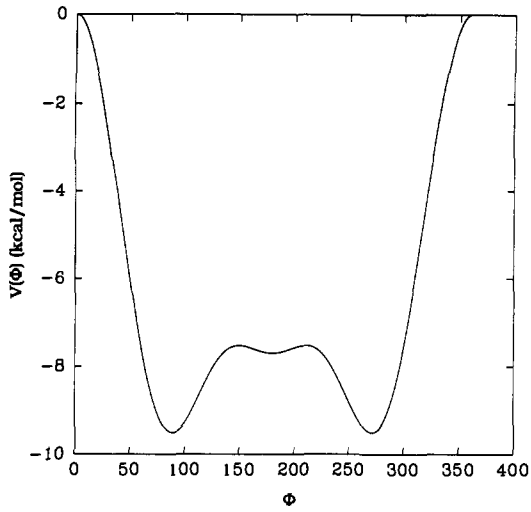

Figure 1. The barrier to internal rotation around the N–N bond obtained from quantum mechanical calculations.

Table II. Charges and Nonbonded Parameters for Hydrazine and CCl_4

solute	charge	R^*, A	ϵ, kcal
N	−0.75	1.900	0.1700
H	0.375	1.000	0.0200
C	0.392	1.7960	0.1013
Cl	−0.098	2.0402	0.3470

basis set.[26] Since ab initio calculations with the 6-31G* basis set are known[27] to overestimate partial charges by a factor of 0.87, we scaled these charges by the same factor. The van der Waals parameters were determined by adjusting them to get the correct density and total energy by doing trial molecular dynamics simulations. These van der Waals parameters along with the partial charges of hydrazine are listed in Table II. The bond lengths and angles of hydrazine used in the calculations were those determined by electron diffraction.[28]

CCl_4 is a simple molecule having a tetrahedral symmetry. The van der Waals parameters for C and Cl atoms of CCl_4 were taken from Evans.[29] The partial charges on the atoms of CCl_4 were obtained by the same method described earlier with both STO-3G and 6-31G* basis sets. It was found that the higher basis set makes carbon more electronegative than chlorine, which is contradictory to the chemical intuition. Therefore, the charges obtained with the STO-3G basis set were used in the present study. These charges and the nonbonded parameters of hydrazine are listed in Table II.

The force field parameters and the partial charges for the solute alkanes and tetraalkylammonium ions are taken from our earlier paper.[1] The van der Waals parameters, R and ϵ for alkali ions (Na^+ and K^+) and halide ions (Cl^- and Br^-) from Lybrand et al.,[30,31] were used in the present study as well as in our earlier study.[2]

Generation of Solvent Boxes. The initial geometry of a hydrazine molecule modeled for the creation of a solvent box has gauche conformation, which has C_2 symmetry. This is usually considered as the equilibrium conformation.[23] A hydrazine molecule has six atomic centers. The solvent molecule with the largest number of atomic centers used in our simulations so far is DMSO, which has 4 atomic centers (the two methyl groups of the DMSO molecules were considered as two centers in a united model representation). The coordinates of the DMSO box were used to generate a hydrazine box in the following way. Two additional centers were generated for each DMSO molecule which are connected to the O atom so that the new molecule will have C_2 symmetry. The S and O positions were substituted by the two N atoms of hydrazine and the other four positions (which include the positions of the two methyl groups of DMSO and the newly generated positions) were substituted by the four hydrogens of hydrazine. The sides of the new box of hydrazine were initially scaled by an appropriate factor to get the right density for hydrazine. This box of 216 hydrazine molecules was minimized by the conjugate gradient method for 5000 cycles, followed by a minimization with SHAKE[32] for an additional 100 cycles. The minimized coordinates were used for molecular dynamics simulations of liquid hydrazine with use of SHAKE and periodic boundary conditions. The time step used in this simulation was 0.001 ps. The trial simulations for obtaining the van der Waals parameters were run for 10–30 ps several times at constant temperature (300 K) and pressure (1 atm). The parameters listed in Table II gave the best results in agreement with the experimental values. For structural analysis, the simulations were run for 100 ps and the coordinates were collected every 0.1 ps. The density and the radial distribution functions (rdfs) of liquid hydrazine were computed from the coordinates over the last 80 ps. The average density of the simulated hydrazine is 1.015 ± 0.010 gm/cm^3, which is in good agreement with the experimental value of 1.00 gm/cm^3.

Table III. The Cutoff Distance and the Number of Solvent Molecules

simulation	solute	ref	solvent	R_c, Å	no. of hydrazine/ CCl_4
1	Cl^-	Br^-	hydrazine	14.0	413
			CCl_4	18.0	292
2	Na^+	K^+	hydrazine	14.0	413
			CCl_4	18.0	292
3	Me_4N^+	NH_4^+	hydrazine	12.0	397
4	Et_4N^+	Me_4N^+	hydrazine	12.0	457
5	C_2H_6	CH_4	hydrazine	14.0	498
			CCl_4	18.0	327
6	Me_4C	CH_4	hydrazine	12.0	397
			CCl_4	18.0	381

The CCl_4 box was created from the water box by generating two additional centers on the central oxygen of water such that the positions of the two oxygens and the the two new centers form a tetrahedron. The position of the O atom at the center of the tetrahedron is substituted by the C atom of CCl_4 and the 4 Cl atoms were placed at the four vertices. The length of the CCl_4 box was initially scaled so as to get the correct density of CCl_4. The bond lengths and angles of CCl_4 molecules were constrained to the experimental values during the present simulation studies. The box of 216 CCl_4 molecules was minimized in two stages as described earlier. Then it was equilibrated at constant temperature (300 K) and pressure (1 atm) for 20 ps by a molecular dynamics run with a time step of 0.001 ps. SHAKE was used during the dynamics run also. Since a great deal of structural information on liquid CCl_4 is available from both the experimental studies[33] and the computer simulation studies,[34] we have not attempted here to analyze our molecular dynamics results in any extensive way except to see that our model gives the correct density and structure. The density of the simulated liquid CCl_4 is 1.5935 ± 0.010 g/cm^3 which is in good agreement with the experimental value of 1.58436. The calculated radial distribution functions are also in good agreement with the experimental and the simulation results.[33,34] The coordinates obtained at the end of the simulation were used for the free energy calculations.

Free Energy Simulations. The solutes were solvated by hydrazine and CCl_4 as described earlier.[1,2,4] The cutoff distance and the number of the solvent molecules solvating each solute are listed in Table III for all transformations. Each system was minimized in four stages. First, the solvent around the solute was minimized for 500 cycles with the steepest descent method. Second, it was minimized for the next 2000 cycles with the conjugate gradient method. Third, the whole system was minimized with the conjugate gradient method for another 1000 cycles followed by a minimization of 100 cycles with SHAKE. The system was initially equilibrated for 10.0 ps at constant temperature (300 K) and pressure (1 atm) with use of a time step of 0.002 ps. During minimization, equilibration, and the subsequent perturbation runs, periodic boundary

(25) QUEST (Version 1.0) by Singh, U. C.; Kollman, P. A.; University of California: San Francisco, 1986.
(26) Hariharan, P. C.; Pople, J. A. *Theor. Chim. Acta* **1973**, *28*, 213.
(27) (a) Singh, U. C.; Kollman, P. A. *J. Comp. Chem.* **1984**, *5*, 129. (b) Cox, S. R.; Williams, D. E. *J. Comp. Chem.* **1981**, *2*, 304.
(28) Kohata, K.; Fukuyama, T.; Kuchitsu, K. *J. Phys. Chem.* **1982**, *86*, 602.
(29) Evans, M. W. *J. Chem. Phys.* **1987**, *86*, 4096.
(30) Lybrand, T. P.; Kollman, P. A. *J. Chem. Phys.* **1985**, *83*, 2923.
(31) Lybrand, T. P.; Indira, G.; McCammon, J. A. *J. Am. Chem. Soc.* **1985**, *107*, 7793.
(32) Ryckaert, J. P.; Ciccotti, G.; Berendsen, H. J. C. *J. Comput. Phys.* **1977**, *23*, 327.
(33) (a) Narten, A. H. *J. Chem. Phys.* **1976**, *65*, 573. (b) Egelstaff, P. A.; Page, D. I.; Powels, J. G. *Mol. Phys.* **1971**, *20*, 881.
(34) (a) Adan, F. S.; Banon, A.; Santamaria, J. *Chem. Phys. Lett.* **1984**, *107*, 475. (b) McDonald, I. R.; Bounds, D. G.; Klein, M. L. *Mol. Phys.* **1982**, *45*, 521. (c) Steinhauser, O.; Neumann, M. *Mol. Phys.* **1980**, *40*, 115. For A RISM study, see: (d) Lowden, L. J.; Chandler, D. *J. Chem. Phys.* **1974**, *61*, 5228.

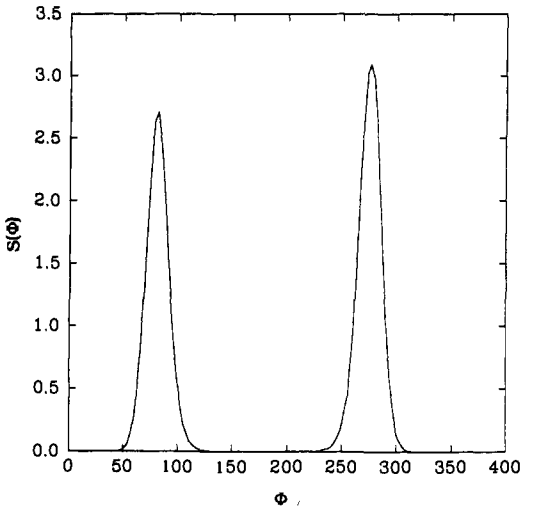

Figure 2. Population densities of different conformers of hydrazine obtained from molecular dynamics over 80 ps.

conditions were applied only for solute–solvent and solvent–solvent interactions. The SHAKE procedure is used during simulation runs also. A constant dielectric of 1 was used for all simulations. Cutoff distances of 12 and 14 Å in hydrazine and CCl_4, respectively, were employed for the nonbonded interactions. All solute–solute nonbonded interactions were included. The nonbonded pair list was updated every 100 molecular dynamics steps. For the transformations involving closed shell ions, 101 windows were employed with 0.4 ps of equilibration followed by 0.4 ps of data collection at each window. For the molecular solutes, the mutation was achieved in two stages with the free energy decoupling method.[1] The partial charges were mutated first by using 21 windows with 1.0 ps of equilibration and 1.0 ps of data collection at each window. The van der Waals parameters were mutated with coordinate coupling over 201 windows with 0.2 ps of equilibration and 0.2 ps of data collection. The time step used during the equilibration and data collection was 0.002 ps.

Results

The molecular dynamics results obtained for the box of 216 hydrazine molecules were analyzed for obtaining the structural information on this liquid. The population densities of different conformers of hydrazine molecules are analyzed to understand the behavior of these molecules in the liquid state, and the radial distribution functions were calculated to get the intermolecular arrangement. A plot of the averaged population densities of hydrazine molecules as a function of the dihedral angle is given in Figure 2. The dihedral angle used for this plot is that between the lone pair positions on the two N atoms of the hydrazine molecule. This shows that most of the 216 molecules stay in the gauche conformation for the duration of the simulation. In other words, the molecule stays in either of the potential wells described in Figure 1. However, several molecules reach the transition structure and stay there for a very short period and then revert back to the initial structure (see Figure 3a), and some molecules roll to the other potential well (see Figure 3b). These results also show that different conformational states of hydrazine molecules are adequately sampled in the present simulation.

(a) Radial Distribution Functions. The radial distribution functions (rdfs) for all intermolecular pairs of atoms of hydrazine are given in Figure 4. As the intramolecular bond distances were constrained, these pairs were not included in the calculated rdfs. The rdf for the N–N pair shows well-defined maxima, whereas the rdfs of N–H and H–H do not show any sharp maxima. The pair distances obtained from the positions of the first one or two maxima in these rdfs are given in Table IV. For some pairs, the coordination numbers were obtained from the areas under the corresponding peaks. These coordination numbers are also given in Table IV. The N–N rdf shows the first maximum at 3.35 Å, a shoulder at 4.10 Å, and a broad maximum at around 7.0 Å. The N–H rdf shows the first small peak at 2.50 Å followed by a broad maximum around 4.0 Å. The H–H rdf raises initially monotonically up to 2.75 Å and then shows a plateau with small

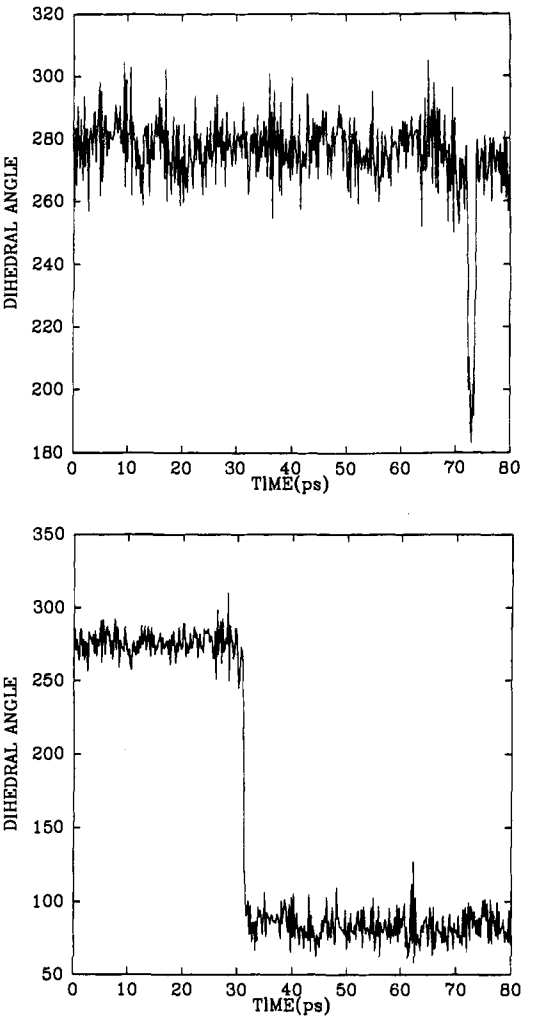

Figure 3. The dihedral angle for a hydrazine molecule as a function of time during the course of the molecular dynamics run. (a) The profile for a molecule that reaches the transition structure for a brief period. (b) The profile for a molecule that crosses the barrier to go from one potential well to the other well.

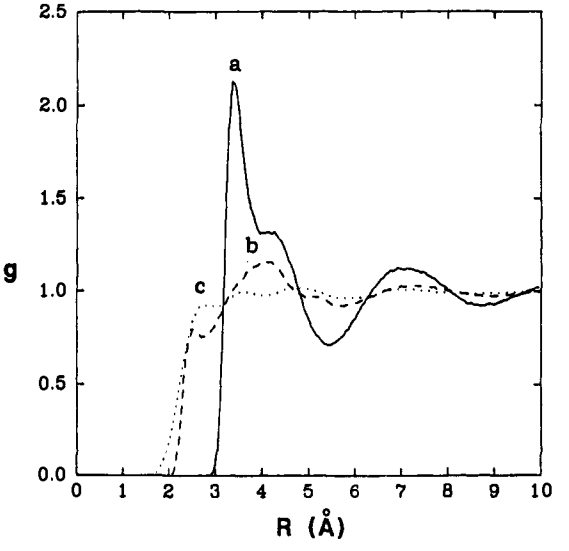

Figure 4. Radial distribution functions of (a) N–N, (b) N–H, and (c) H–H pairs of liquid hydrazine.

fluctuations. The two broad maxima may be located around 3.6 and 4.5 Å following the initial peak in the H–H rdf. The integration of the N–N peak up to the shoulder gives a coordination number of 8.5. When the integration is extended up to the first real minimum at 5.45 Å, then the coordination number is 24.5.

Table IV. Pair Distances and Coordination Numbers (CN)

pair	distance, Å	CN[a]
N–N	3.35	8.5 (3.95)
	4.10	24.5 (5.45)
N–H	2.50	2.10 (2.7)
	4.05	
H–H	2.75	
	3.6	

[a] The values in parentheses are the cutoff distances used in the integration of the first peaks of the rdfs to get the coordination numbers.

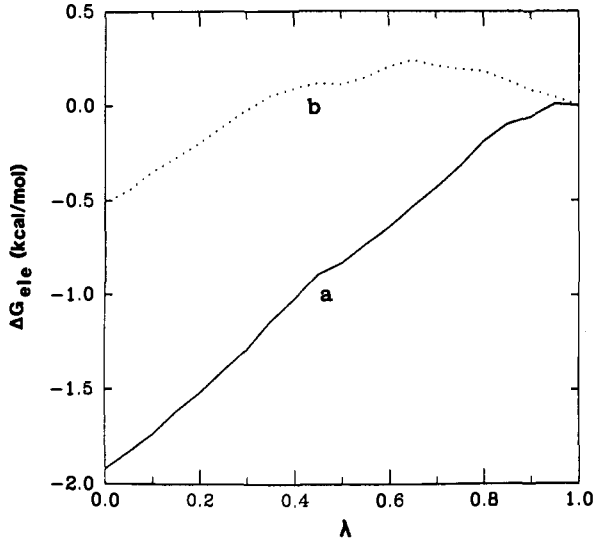

Figure 5. Variation of ΔG_{ele} with λ for transformations in hydrazine and CCl_4: (a) $Me_4N^+ \rightarrow NH_4^+$ in hydrazine; (b) $Et_4N^+ \rightarrow Me_4N^+$ in hydrazine.

The integration of the N–H peak at 2.5 Å gives a coordination number of 2.10.

(b) Free Energy Differences. The calculated free energy differences and the experimental values from the literature for all the transformations are summarized in Table V. For each transformation, the electrostatic part, ΔG_{ele}, and the van der Waals part calculated with coordinate coupling, $\Delta G_{vdw/cc}$, and their sum are listed. The reported ΔG_{ele} and $\Delta G_{vdw/cc}$ values are the averages of the values obtained from the forward and the backward simulations. The data for different transformations in water are taken from our earlier papers.[1,2] For all cases, the dominant contribution to the total free energy difference comes from the $\Delta G_{vdw/cc}$ term. The ΔG_{ele} values are very small in most cases and are almost negligible for neutral alkanes. The experimental values available in the literature[35] are listed for comparison in the last column of Table V. The calculated solute–solvent interaction energies for the solutes in the three solvents are given in Table VI.

For neutral alkanes, ΔG_{ele} varies very little with λ. The values of ΔG_{ele} for the transformations of these solutes are smaller than 0.1 kcal/mol in most cases. For positively charged alkylammonium ions in hydrazine, however, ΔG_{ele} decreases with λ. The variations of ΔG_{ele} with λ for the two transformations involving these ions in hydrazine are shown in Figure 5. The ΔG_{ele} decreases to −1.94 and −0.54 kcal/mol for the $Me_4N^+ \rightarrow NH_4^+$ and the $Et_4N^+ \rightarrow Me_4N^+$ transformations, respectively. These values are also small compared to the corresponding $\Delta G_{vdw/cc}$ values for the same transformations.

The variation of $\Delta G_{vdw/cc}$ with λ for the transformation of $Cl^- \rightarrow Br^-$ in water, hydrazione, and CCl_4 is given in Figure 6. In all three solvents, $\Delta G_{vdw/cc}$ increases linearly with λ. However, the rate of increase in $\Delta G_{vdw/cc}$ is lower in CCl_4 than in water and hydrazine. The final values of $\Delta G_{vdw/cc}$ in hydrazine and CCl_4 are 2.65 and 0.71 kcal/mol. The variation of $\Delta G_{vdw/cc}$ with λ for the transofmration of $Na^+ \rightarrow K^+$ in water, hydrazine, and CCl_4 is given in Figure 7. In this case also, $\Delta G_{vdw/cc}$ increases linearly

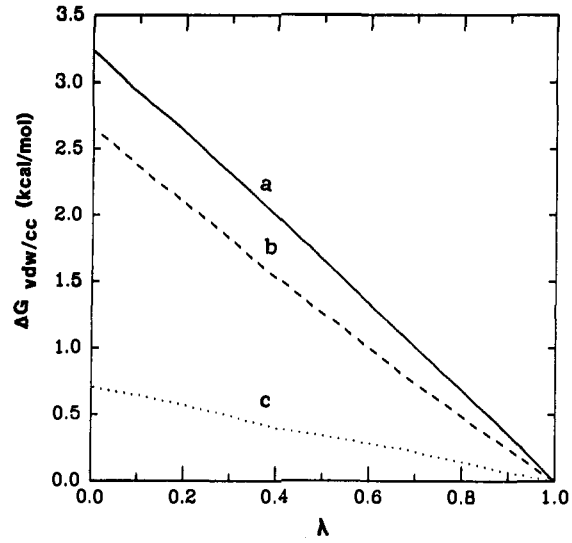

Figure 6. Variation of $\Delta G_{vdw/cc}$ with λ for $Cl^- \rightarrow Br^-$ transformation in (a) water, (b) hydrazine, and (c) CCl_4.

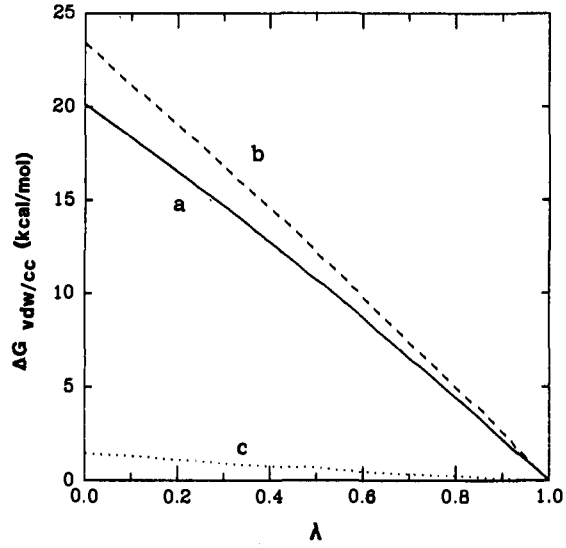

Figure 7. Variation of $\Delta G_{vdw/cc}$ with λ for $Na^+ \rightarrow K^+$ transformation in (a) water, (b) hydrazine, and (c) CCl_4.

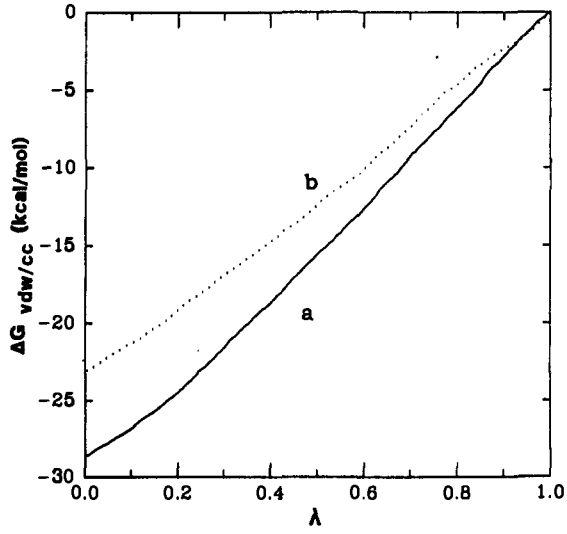

Figure 8. Variation of $\Delta G_{vdw/cc}$ with λ for $Me_4N^+ \rightarrow NH_4^+$ transformation in (a) water and (b) hydrazine.

(35) Free energy values for solvation of alkali ions and halide ions are taken from: (a) Izmailov, N. A. *Dokl. Akad. Nauk. SSSR* **1963**, *149*, 1364. The values for alkanes in CCl_4 are taken from: (b) Abraham, M. H. *J. Am. Chem. Soc.* **1982**, *104*, 2085.

Table V. Calculated and Experimental Free Energy Changes[a]

solute	ref	solvent	ΔG_{ele}	$\Delta G_{vdw/cc}$	total	expt
Cl^-	Br^-	H_2O		3.23 ± 0.05	3.23 ± 0.05	3.3
		hydrazine		2.65 ± 0.37	2.65 ± 0.37	2.5
		CCl_4		0.71 ± 0.04	0.71 ± 0.04	
Na^+	K^+	H_2O		20.09 ± 0.07	20.09 ± 0.07	17.5
		hydrazine		23.32 ± 0.11	23.32 ± 0.11	17.0
		CCl_4		1.46 ± 0.03	1.46 ± 0.03	
Me_4N^+	NH_4^+	H_2O	−0.65 ± 0.00	−29.17 ± 0.52	−29.82 ± 0.52	−31.7
		hydrazine	−1.94 ± 0.02	−23.60 ± 0.33	−25.54 ± 0.35	
Et_4N^+	Me_4N^+	H_2O	−0.64 ± 0.01	−6.10 ± 0.25	−6.74 ± 0.26	−7.0
		hydrazine	−0.54 ± 0.03	−3.62 ± 0.25	−4.16 ± 0.28	
C_2H_6	CH_4	H_2O	−0.09 ± 0.01	−0.33 ± 0.02	−0.42 ± 0.03	0.2
		hydrazine	−0.11 ± 0.01	0.74 ± 0.04	0.67 ± 0.05	
		CCl_4	−0.01 ± 0.01	1.09 ± 0.04	1.08 ± 0.05	1.2
Me_4C	CH_4	H_2O	−0.05 ± 0.01	−0.81 ± 0.07	−0.86 ± 0.08	−0.5
		hydrazine	0.03 ± 0.01	3.61 ± 0.06	3.64 ± 0.07	
		CCl_4	0.00 ± 0.00	3.53 ± 0.17	3.53 ± 0.17	

[a] All values are in kcal/mol.

Table VI. Interaction Energies of Solutes in Water, Hydrazine, and CCl_4[a]

solute	H_2O	hydrazine	CCl_4
Cl^-	−134.3 ± 5.7	−114.3 ± 2.6	−5.0 ± 1.3
Br^-	−132.2 ± 5.0	−106.4 ± 2.4	−5.5 ± 0.4
Na^+	−195.7 ± 8.8	−189.8 ± 5.5	−3.9 ± 0.9
K^+	−155.6 ± 7.5	167.8 ± 4.0	−4.2 ± 0.8
NH_4^+	−138.5 ± 6.4	−151.7 ± 4.9	
Me_4N^+	−100.2 ± 7.0	−113.5 ± 5.6	
Et_4N^+	−96.7 ± 5.9	−105.6 ± 4.5	
CH_4	−2.8 ± 0.6	−4.6 ± 0.7	−3.5 ± 0.3
C_2H_6	−4.9 ± 0.7	−6.5 ± 0.7	−6.0 ± 0.8
Me_4C	−8.4 ± 0.8	−12.9 ± 0.7	−11.7 ± 0.7

[a] All values are in kcal/mol.

with λ. The rate of increase in $\Delta G_{vdw/cc}$ is highest in hydrazine, which is closely followed by that in water. In contrast, the increase in $\Delta G_{vdw/cc}$ in CCl_4 is very marginal. The final $\Delta G_{vdw/cc}$ values are 23.32 and 1.46 kcal/mol respectively in hydrazine and CCl_4.

The variation of $\Delta G_{vdw/cc}$ with λ for the transformation of $Me_4N^+ \rightarrow NH_4^+$ in water and hydrazine is given in Figure 8. This transformation in CCl_4 is not simulated. The $\Delta G_{vdw/cc}$ decreases linearly and the rate of decrease is slightly lower in hydrazine than in water. The final $\Delta G_{vdw/cc}$ value in hydrazine is −23.60 kcal/mol and the corresponding total free energy difference is −25.54 kcal/mol. The variation of $\Delta G_{vdw/cc}$ with λ for transformation of $Et_4N^+ \rightarrow Me_4N^+$ in water and hydrazine is given in Figure 9. This transformation is also not simulated in CCl_4. The $\Delta G_{vdw/cc}$ initially decreses more sharply than in the later part of the transformation. This pattern is more striking in hydrazine than in water. The final $\Delta G_{vdw/cc}$ value in hydrazine is −3.62 kcal/mol and the corresponding total free energy changes are −6.74 and −4.16 kcal/mol in water and hydrazine, respectively.

The variation of $\Delta G_{vdw/cc}$ with λ for the transformation of $C_2H_6 \rightarrow CH_4$ in water, hydrazine, and CCl_4 is given in Figure 10. In CCl_4, the $\Delta G_{vdw/cc}$ increases almost linearly, whereas it initially decreases in hydrazine and then increases later almost parallel to the curve corresponding to CCl_4. In contrast, the curve for water shows a broad dip. The final $\Delta G_{vdw/cc}$ values are 0.74 and 1.09 kcal/mol in hydrazine and CCl_4, respectively. The corresponding total free energy differences are 0.67 and 1.08 kcal/mol, respectively. For the $Me_4C \rightarrow CH_4$ transformation, the variation of $\Delta G_{vdw/cc}$ versus λ, shown in Figure 11, is qualitatively similar to that of the $C_2H_6 \rightarrow CH_4$ transformation. However, the pattern of the curve in hydrazine is close to that in CCl_4 than to that in water. The final values of $\Delta G_{vdw/cc}$ are 3.61 and 3.53 kcal/mol in hydrazine and CCl_4, respectively. The corresponding total free energy differences are 3.64 and 3.53 kcal/mol.

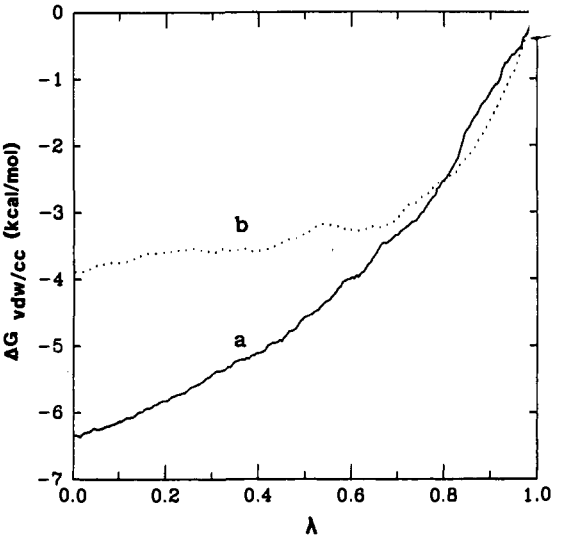

Figure 9. Variation of $\Delta G_{vdw/cc}$ with λ for $Et_4N^+ \rightarrow Me_4N^+$ transformation in (a) water and (b) hydrazine.

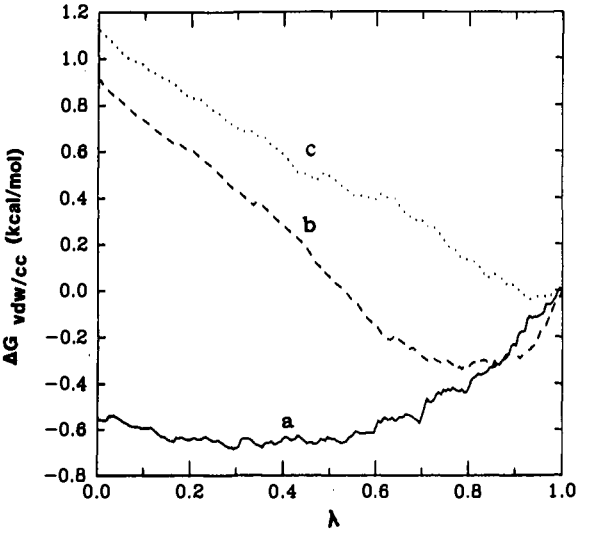

Figure 10. Variation of $\Delta G_{vdw/cc}$ with λ for $C_2H_6 \rightarrow CH_4$ transformation in (a) water, (b) hydrazine, and (c) CCl_4.

Discussion

(a) Radial Distribution Functions for Liquid Hydrazine. It is very striking that the positions of the two major maxima in the calculated rdf of the N–N pair in liquid hydrazine coincide with those of the experimental N–N rdf in liquid ammonia.[36] Similar expeirmental data are not available for liquid hydrazine in the literature. The present results show that the intermolecular correlations in liquid ammonia and liquid hydrazine are quite similar. Therefore a detailed comparison of the present results

(36) Narten, A. H. *J. Chem. Phys.* **1977**, *66*, 3117.

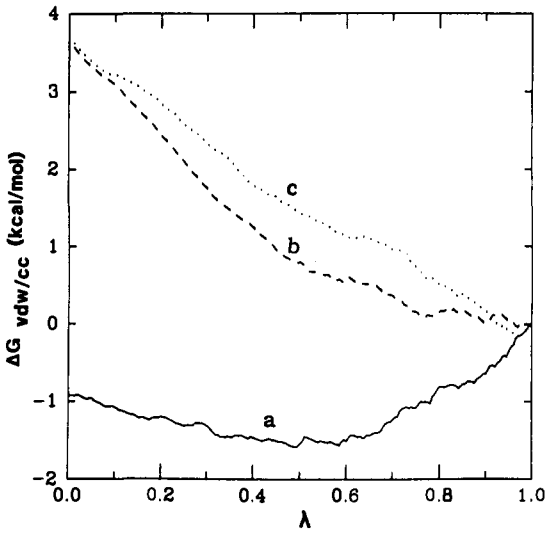

Figure 11. Variation of $\Delta G_{vdw/cc}$ with λ for $Me_4C \rightarrow CH_4$ transformation in (a) water, (b) hydrazine, and (c) CCl_4.

with the X-ray diffraction results on liquid ammonia is expected to bring out the similarities and differences in the structures of these two liquids. The experimental rdf for the N–N pair in liquid ammonia has its first maximum at 3.4 Å, followed by a shoulder at 3.7 Å, and a subsidiary maximum at 4.6 Å. Additionally, there is a broad maximum around 7 Å. The maxima at 3.4 and 3.7 Å were attributed to the N–N pairs making hydrogen bonds and van der Waals contacts, respectively. The peak at 4.6 Å is attributed to N–N pairs not making either of the above interactions, but being in the first coordination. In contrast, the N–N rdf in liquid hydrazine is indicative of only two kinds of N–N pairs in the first coordination sphere. The snap shot picture of the equilibrated box of 216 hydrazine molecules shown in Figure 12 reveals that the coordination around a hydrazine molecule in the liquid state is complex. The configuration shown in the figure is obtained at the end of the 100-ps simulation run. An examination of this structure shows that each N atom has both hydrogen-bonded and non-hydrogen-bonded neighbors. The shoulder at 4.1 Å following the first maximum in the rdf of hydrazine may be associated with the N–N pairs that are not hydrogen bonded. This is, however, mainly a consequence of the nature of the hydrazine molecule, in which two N atoms are bonded. When two hydrazine molecules are hydrogen bonded, only one N atom on each molecule is involved in this interaction, for which the pair correlation appears around 3.4 Å in the rdf curve. An additional well-defined N–N correlation around 4 Å is expected in this configuration, in which the first N atom in the N–N pair belongs to the first molecule and is involved in hydrogen bonding and the second N atom of the pair is that of the second molecule which is not involved in hydrogen bonding. Such a pair correlation is depicted schematically in Figure 13. When the first peak is integrated up to the beginning of the shoulder in the N–N rdf of hydrazine, it shows that about 8 N atoms coordinate an N atom in a distance range of 3.1–3.95 Å. Since the intramolecular N–N distance is 1.45 Å, all 8 N atoms may belong to 4 hydrazine molecules. The integration of the first peak up to the first real minimum distance in the rdf gives a coordination number of about 24. This suggests that an N atom of a hydrazine molecule is coordinated by at least 12 hydrazine molecules. It should be noted that most of these 12 molecules are also in the first coordination of the second N atom of the same central hydrazine molecule. Therefore, these results show that each hydrazine molecule in the liquid state is surrounded by at least 12 other hydrazine molecules. The well-defined maximum around 7 Å observed in the N–N rdfs of ammonia and hydrazine suggests a significant degree of order in the two liquids.

The rdfs of the N–H and H–H pairs in liquid hydrazine look similar to the rdfs of the same pairs in liquid ammonia obtained from the computer simulation studies.[37,38] The experimental information on N–H and H–H pair correlations in liquid ammonia is not available. The rdf of the H–H pair is almost structureless for both liquids. This rdf has broad peaks at 3.75 and 4.1 Å in liquid hydrazine. The N–H pair rdfs show a clearly defined first peak at 2.5 Å, which is indicative of hydrogen bonding between these molecules in the liquid state. The integration of this peak up to 2.7 Å shows that there are about two hydrogen bonds on each N atom of each hydrazine molecule. Similar results were obtained for the N–H pair in the computer simulation study[38] on liquid ammonia as well.

Some of the structural features of liquid hydrazine noted so far are also common with those of water. In particular, hydrogen bonding seems to be an important factor in both of these liquids and the number of hydrogen bonds per molecule is about four in both cases. The H–H rdfs of hydrazine indicate a coordination number of 5.7 which is close to that in water.[39] However, the first peak in the N–H rdf in liquid hydrazine is not so well defined as the peak in the O–H rdf of liquid water,[39] suggesting that hydrogen bonds in liquid hydrazine are not as strong as those in water. The present analysis of the structure of liquid hydrazine is not complete and it is not yet possible to say if there is any network of hydrogen bonds in liquid hydrazine as found in water. The examination of Figure 12, however, shows that the coordination around a hydrazine molecule in liquid is much more complex than that in water. Clearly the present model structure of hydrazine shows features common with both liquid water and liquid ammonia and it resembles the structure of liquid ammonia more closely than that of liquid water. Therefore, the behavior of hydrazine as a solvent is expected to be close to that of ammonia in most of the cases discussed in the next section. If any differences are observed between the solvation of apolar solutes in water and hydrazine, those differences may be attributed to the differences in the structures of the liquids noted in this section.

(b) Free Energy Differences. The calculated free energy difference for $Cl^- \rightarrow Br^-$ transformation in hydrazine agrees well with the experimental value. It may be noted here that the parameters used for these anions are the same as those used in our earlier study, in which the free energy difference for the same transformation in water was calculated to be 3.23 kcal/mol which is closer to the experimental value reported by Krishnan and Freedman[40] (3.3 kcal/mol) and is smaller than that reported by Marcus[41] (6.2 kcal/mol). It is interesting that the parameters optimized to reproduce the experimental value in water reported by Freedman and Krishnan estimates correctly the difference in free energy of solvation of these two ions in hydrazine. The calculated free energy difference for this transformation in CCl_4 is much smaller (0.71 kcal/mol) than in water or hydrazine. This is clearly due to the fact that the ion–solvent interaction energies are much smaller in CCl_4 than in water or hydrazine. This also explains why CCl_4 is not a good solvent for anions. Further, the interaction energies of these two ions in CCl_4 are almost equal to each other whereas the interaction energy of the Cl^- ion is lower than that of the Br^- ion in hydrazine. Therefore, the calculated free energy difference for the two ions in CCl_4 is much smaller than that in hydrazine or water. This is depicted in the rate of change of $\Delta G_{vdw/cc}$ with λ shown in Figure 6, for the three solvents. The rate is high in water and hydrazine compared to CCl_4. It shows that the nature of interaction of these ions in water and hydrazine is similar. The Cl^- interacts with hydrazine through a hydrogen bond as in water, but the strength of this interaction is lower in hydrazine than in water since hydrazine is not as good a hydrogen bond donor as water. No such specific interaction is possible between the Cl^- ion and CCl_4. Liquid CCl_4 is like a low-dielectric, hard-sphere solvent with higher probability of larger

(37) Hinchliffe, A.; Bounds, D. G.; Klein, M. L.; McDonald, I. R.; Righini, R. *J. Chem. Phys.* **1981**, *74*, 1211.
(38) Sagarik, K. P.; Ahlrichs, R.; Brode, S. *Mol. Phys.* **1986**, *57*, 1247.
(39) (a) Palinkas, G.; Kalman, E.; Kovacs, P. *Mol. Phys.* **1977**, *34*, 525. (b) Soper, A. K.; Silver, R. N. *Phys. Rev. Lett.* **1982**, *49*, 471.
(40) Freedman, H. L.; Krishnan, C. V. In *Water—A Comprehensive Treatise*; Franks, F., Ed.; Plenum Press: New York, 1973; Vol. 3, p 1.
(41) Marcus, Y. *Ion Solvation*; John Wiley & Sons: New York, 1985; p 108.

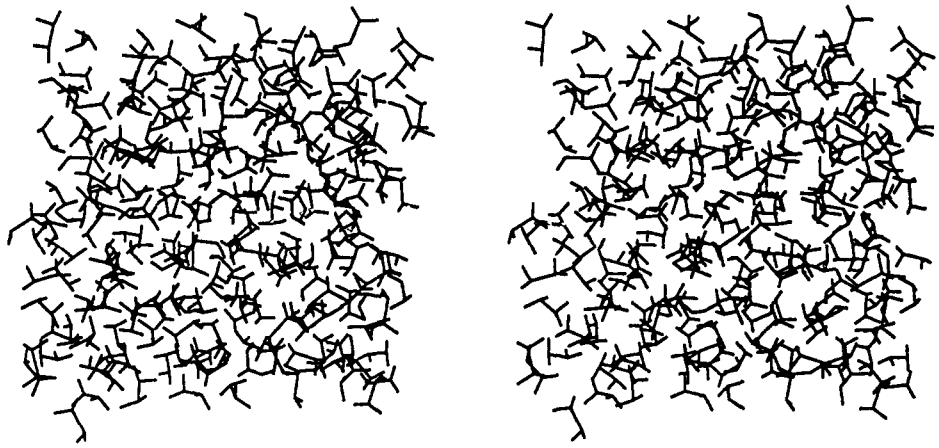

Figure 12. Stereopicture of 216 hydrazine molecules at the end of the 100-ps molecular dynamics run. The solvent boxes of hydrazine and CCl_4 were made as described in the text.

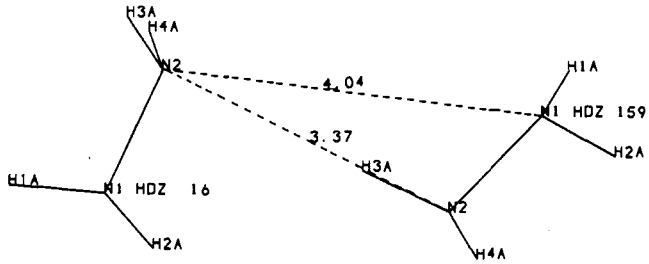

Figure 13. A schematic representation of different pair correlations between two hydrogen-bonded hydrazine molecules.

cavity sizes than in water[10] and hence CCl_4 does not differentiate between the two ions either by any specific interaction or by the size difference of the two ions.

For the transformation of $Na^+ \rightarrow K^+$ in hydrazine, the calculated free energy difference is slightly overestimated. According to the present calculation, the difference in the free energy of solvation between the two cations is slightly larger in hydrazine than in water, though the experimental values are almost equal. The calculated free energy difference for this transformation in CCl_4 is much smaller than that in water or hydrazine. This is again due to negligibly small ion–solvent interaction energies in CCl_4, which are almost equal for the two cations. Further, the interaction energies for the cations in CCl_4 are only slightly smaller than those for the anions suggesting that the nature of the charge on the solute has little effect on the interaction of these solute ions with CCl_4. The interaction between ions and CCl_4 is mainly due to ion–octopole interactions, whereas the interaction of ions with water and hydrazine is dominated by strong ion–dipole interaction. It may be noted here that dipole moments of water and hydrazine are almost equal, whereas CCl_4 has no dipole moment. The change in the solute size affects the solute–solvent interaction energies to a greater extent in water and hydrazine than in CCl_4, which is reflected in the variation of ΔG_{vdw} versus λ shown in Figure 7.

For the $Me_4N^+ \rightarrow NH_4^+$ transformation, the calculated free energy difference is smaller in hydrazine (−25.54 kcal/mol) than in water (−29.82 kcal/mol). Similarly for the $Et_4N^+ \rightarrow Me_4N^+$ transformation, the calculated free energy difference is smaller (−4.16 kcal/mol) than that in water (−6.74 kcal/mol). No experimental values are available for these transformations in hydrazine. However, if we take the trend of solvation of other cations in hydrazine[35] as compared to water as a guide, it is expected that the free energy changes for these transformations in hydrazine will be almost the same or slightly smaller than those in water. The present results are in qualitative agreement with the observed trend. For these transformations in water and hydrazine, an examination of the variation pattern of $\Delta G_{vdw/cc}$ versus λ shown in Figures 8 and 9, respectively, leads to the following three observations: (a) $\Delta G_{vdw/cc}$ for this transformation decreases continuously with λ. (2) The rate of decrease in $\Delta G_{vdw/cc}$ is initially higher than that in the later part of the transformation. (3) The rate of decrease at higher values of λ is higher in water than in hydrazine. The continuous decrease in $\Delta G_{vdw/cc}$ observed for these transformations seems to result from large differences in interaction energies. For the first transformation, the interaction energy decrease by about 38 ± 6 kcal/mol in both solvents. For the second transformation, the decrease in interaction energy is only marginal (about 5 kcal/mol) in the two solvents. The important observation to be made here is that the decrease in the free energy for the two transformations in water is larger than that in hydrazine, though the decrease in the interaction energies for these transformations in the two solvents is almost the same. It is reasonable to assume that an additional factor contributes to the free energy change for transformations in water. These observations were made in our earlier study[2] also, where the behavior in water is compared with that in MeOH and DMSO. The behavior in water was explained by presuming that the water molecules around the solute are "repulsed" by the hydrophobic methyl groups and form a strongly bound solvation shell around the solute in accordance with Frank and Evans' hypothesis.[5] Because of the presence of the unit positive charge of tetraalkylammonium ions, the solvent is strongly pulled toward the solute which results in configurations wherein the solute and the surrounding solvent are further pushed into the repulsive region of the solute–solvent interaction potential surface. Since the van der Waals interaction due to four methyl groups is made to disappear during mutation, the repulsive solute–solvent interaction is relieved and the tight water structure around the solute is loosened. Alternatively, it may be conceived that reduction of the van der Waals size and well depth parameters has the effect of increasing the temperature locally around the perturbed solute in the system and the structure of the solvent cage around the solute is progressively disrupted on increasing this fictitious temperature causing an increase in entropy of the system. Therefore, the free energy decreases aided by both decrease in interaction energy and increase in entropy due to solvent reorganization. The larger decrease in free energy for the two transformations in water may be attributed to the contribution due to the reorganization of the tightly bound solvent cage around these solutes in water. The results for hydrazine suggest that such a tightly bound solvent cage around the tetraalkylammonium ions is not as strong as in water. For tetraalkylammonium ions, the behavior of hydrazine as a solvent seems to be somewhat different from that of water.

For the $C_2H_6 \rightarrow CH_4$ transformation in CCl_4, the agreement between the calculated free energy difference and the experimental value is surprisingly good. For this transformation in water, the calculated value was not in good agreement with the experimental value. The experimental value for this transformation in hydrazine is not available for comparison. The discrepancy between the calculated and the experimental values in water was explained[1] as due to very small interaction energies of these molecules with

water (Table VI) and to the unsymmetric change in the shape of the solute molecule with mutation. Since water forms a strongly bound solvent shell round apolar solutes, it is possible that water may not reorganize fast enough from a peanut shaped solvent shell around ethane to a spherical solvent shell around methane. It may be easier for CCl_4 to reorganize during this transformation as these solvents may not form a tight solvent shell around these solutes. Hence the error caused by the unsymmetric nature of the transformation may be less in CCl_4 than in water. The experimental values for the $Me_4C \rightarrow CH_4$ transformation in hydrazine and CCl_4 are not available in the literature. For these two transformations involving alkanes, $\Delta G_{vdw/cc}$ in CCl_4 increases almost linearly. In hydrazine, however, the variation of $\Delta G_{vdw/cc}$ is different in the two transformations. For the $C_2H_6 \rightarrow CH_4$ transformation, $\Delta G_{vdw/cc}$ decreases initially as λ varies from 1.0 to around 0.8 and then it increases almost parallel to the curve for the same transformation in CCl_4. For the $Me_4C \rightarrow CH_4$ transformation, $\Delta G_{vdw/cc}$ increases almost monotonically, but the rate of increase is lower initially than in the later stage of the transformation. In water, $\Delta G_{vdw/cc}$ initially decreases until λ is between 0.7 and 0.5 and then it increases. The behavior of the two transformations in hydrazine does not completely resemble the behavior noted for water, nor does it resemble that observed in CCl_4. The interaction energies of these solutes in water are lower than those in hydrazine and CCl_4. Nevertheless, the interaction energy increases with decreasing size of the solute in each case. The change in the interaction energy for the $C_2H_6 \rightarrow CH_4$ transformation is almost the same (about 2 kcal/mol) in all three solvents, whereas the change in the interaction energies for the $Me_4C \rightarrow CH_4$ transformation is smaller in water (about 4 kcal/mol) than in hydrazine or CCl_4 (about 6 kcal/mol). If the enthalpic term has dominant contribution to the change in free energy of these transformations, then the free energy should continuously increase in all cases. Such an increase is indeed observed in CCl_4, and also in MeOH and DMSO reported in our previous study.[2] Though the interaction energies for three alkanes in hydrazine are almost equal to those in CCl_4, the behavior of the two transformations in hydrazine does not resemble that in CCl_4. This may be indicative of a solvent cage around these solutes in hydrazine similar to the solvent cage around apolar solutes in water. Note that the behavior in water, with a dip in the variation of $\Delta\Delta G_{vdw/cc}$, has been explained as resulting form the reorganization of the tightly bound water cage around the apolar solutes. For the first transformation for this series in hydrazine, a clear dip is observed in Figure 10. Though no dip is observed for the second transformation ion hydrazine, the shape of the curve for hydrazine in Figure 11 around $\lambda = 0.8$ shows a marked departure form the linearity observed for the curve of CCl_4. It must be noted, however, that the change in interaction energies for the second transformation is larger than that for the first one. Hence, the relative contribution of the enthalpic term compared to the entropic term to the free energy change is larger in the second transformation. The present data show that the signature of the structural effect noted for the behavior of alkanes in water is also present in hydrazine and the magnitude of this effect is definitely smaller in hydrazine than in water. No such effect is observed for CCl_4.

Conclusions

The structure of a model of liquid hydrazine has been obtained for the first time with use of molecular dynamics simulations and compared with the structures of liquid ammonia and water. The simulation results show that hydrazine molecules in the liquid state are associated through hydrogen bonding as in liquid ammonia and water. These results also indicate that the molecular arrangement in liquid hydrazine is ordered to a significant degree even beyond the first coordination sphere. However, the hydrogen bonding in liquid hydrazine is not found to be as extensive as in water. The molecular arrangement in liquid hydrazine seems to be closer to that in liquid ammonia than in liquid water.

The calculated free energy changes and interaction energies are affected by the size of ionic solutes, like small anions and cations, and tetraalkylammonium ions to a similar extent in water and hydrazine. In CCl_4, these ionic solutes are very weakly interacting and the nature of the charge and the size of the solute ions have only marginal effect on the free energy change in this liquid. The characteristic feature of hydrophobicity observed in the variation patterns of free energy change for alkanes and large tetraalkylammonium ions in water is not observed in CCl_4. On the other hand, the variation patterns of $\Delta G_{vdw/cc}$ observed for the mutations of alkanes in hydrazine resemble those in water hydrogen bonds among the solvent molecules. These aspects of solvation in liquid hydrazine need further investigation before a firm conclusion is drawn about the nature of the solvation shell. The present study suggests that the hydrophobic effect arises mainly from the structural features of water that are common with those of liquid hydrazine. We hope that the present work provides an impetus for further experimental research in this important area of nonaqueous solvation.

Acknowledgment. All calculations were performed on the CRAY X-MP/116SE supercomputer at the Research Institute of Scripps Clinic. We are grateful to Dr. Richard A. Lerner for providing the computer facilities and encouragement. This research is partially supported by a grant from the National Institutes of Health (R01-GM 39410).

Registry No. CCl_4, 56-23-5; hydrazine, 302-01-2.